

Feedback Control of a Biodynamical Model of HIV-1

Michael E. Brandt*, *Member, IEEE*, and Guanrong Chen, *Fellow, IEEE*

Abstract—We describe a continuous differential equation model of the interaction dynamics of HIV-1 and CD4 and CD8 lymphocytes in the human body. We demonstrate several methods of stable control of the HIV-1 population using an external feedback control term that is analogous to the introduction of a therapeutic drug regimen. We also show how the immune system components can be bolstered against the virus through a feedback control approach.

Index Terms—Antiretroviral therapy, feedback control, HIV infection, nonlinear modeling.

I. INTRODUCTION

OVER the last several years, significant progress has been made in our understanding of the pathogenesis of human HIV infection [1]. The insights derived from research have led to new therapeutic paradigms including “highly active antiretroviral therapy” (HAART) drug regimens. In HAART, three or more antiretroviral agents are taken in combination by the patient, often up to three times daily [2]–[4]. Currently, there are 15 FDA-approved medications available for HIV infection.

During the primary infection of HIV, large numbers of cells in the body are rapidly affected which leads to high titers of infectious virions measured in blood plasma [5]. These titers have been known to be as high as 10^7 /ml of plasma [6]. Following the primary infection, the number of infectious virus particles in plasma drops to almost undetectable levels as virus-specific immunity develops in the host [7]. Despite this precipitous drop of virus in the blood, it is now known that HIV replication continues unchecked within the lymphatic system [8], [9] and possibly in other tissues such as the nervous system contributing to a latent stage of infection.

HIV-1 (the predominant HIV strain in the West), is a highly dynamic disease [10], [11]. It is estimated that as many as 10^{10} HIV-1 virions are produced and destroyed in an infected individual each day [12]. This is coupled with the production and destruction of approximately 2×10^{10} CD4+ immune system lymphocytes (the main target of the virus)/day. The half-life of HIV-1 in plasma is on the order of minutes to 1 day. The main hallmark of HIV infection leading to full-blown AIDS is high levels of virus in the blood together with decreasing numbers of CD4+ lymphocytes [13].

There is a second, slower phase of infection with a half-life of approximately 14 days, followed by a third phase of infection

with a half-life of about 5–6 months [14]. There may even be additional hidden reservoirs of virus, such as in the central nervous system that contribute to an even slower disease phase. These additional phases of infection make complete eradication of the virus from the body all but impossible with currently available therapies. Furthermore, the constant turnover of the virus population under therapeutic pressure drives genetic mutation of the virus which provides a mechanism for the rapid evolution of drug resistant strains [15]. Thus, current treatment guidelines require the use of aggressive adherence to HAART in order to keep the levels of virus measured in plasma as low as possible.

Adherence to HAART however, is a significant problem—many patients have trouble with the dosing requirements and side-effects of such therapy can be severe. A regimen that could reduce dosage requirements while maintaining control over viral plasma levels might not only increase patient adherence but the overall health of the patient by reducing side effects. In the following, we describe a nonlinear continuous differential equation model of the interaction dynamics of HIV-1, and CD4+ and CD8+ lymphocyte counts in the body. Using this model, we perform studies to simulate a therapeutic drug regimen based on time-delay feedback control to suppress the virus to undetectable levels.

II. DESCRIPTION OF THE MODEL

The nonlinear dynamical model of HIV-1 is a predator–prey model in the form [16]

$$\begin{aligned}\dot{x} &= a(x_0 - x) - bxz \\ \dot{y} &= c(y_0 - y) + dyz \\ \dot{z} &= z(ex - fy)\end{aligned}\quad (1)$$

where

x	CD4 lymphocyte population;
x_0	normal, unperturbed CD4 count;
y	CD8 lymphocyte population;
y_0	normal, unperturbed CD8 count;
z	HIV-1 viral load;
a – f	parameters.

Several facts are known concerning the interaction of the HIV-1 virus and the immune lymphocytes CD4 and CD8:

- 1) HIV-1 utilizes CD4 cells to replicate itself, and their growth rates are inversely proportional.
- 2) The growth rate of CD8 cells increase in response to increased HIV-1 load, and CD8 cells attack the virus.
- 3) The growth rate of HIV-1 increase with increased growth in the HIV-1 and CD4 populations.
- 4) The growth rate of HIV-1 decreases with decreased growth in the HIV-1 and CD4 populations.

Manuscript received April 24, 2000; revised April 6, 2001. Asterisk indicates corresponding author.

*M. E. Brandt is with the Neurosignal Analysis Laboratory in the School of Health Information Sciences, University of Texas Health Science Center, 7000 Fannin St., Suite 600, Houston, TX 77030 USA (e-mail: Michael.E.Brandt@uth.tmc.edu).

G. Chen is with the Department of Electrical and Computer Engineering, University of Houston, Houston, TX 77030 USA.

Publisher Item Identifier S 0018-9294(01)05133-3.

In principle, the parameters b and e are controlled by HIV-1, and a , c , d , and f are subject to manipulation in an effort to reduce the viral load. The goal of this study is to explore various options for controlling the virus production rate using feedback control strategies. In such strategies, state variables which are periodically sampled, are used to vary the treatment regimen on an ongoing basis. This control method is reminiscent of target tracking in general, an example of which is thermostatic regulation.

III. METHOD AND RESULTS

The system (1) has two equilibrium points. The first corresponds to the unstable point $x^* = x_0$, $y^* = y_0$, $z^* = 0$. The second equilibrium point can be determined by noting that

$$\begin{aligned} x^* &= ax_0/(a + bz^*) \\ y^* &= cy_0/(c - dz^*) \\ 0 &= z^*(ex^* - fy^*). \end{aligned} \quad (2)$$

With $z^* \neq 0$, algebraic manipulation of these three relations yields

$$z^* = \frac{ac(ex_0 - fy_0)}{adex_0 + bcfy_0}. \quad (3)$$

One observes from these relations that the internal dynamics of z^* are largely determined by the parameters e and f (z^* will decrease if f is increased at the expense of e). Note that z^* can also be decreased by increasing b and d and/or by decreasing a and c (of these only b is virus-dependent).

One can also introduce an external control agent (e.g., an antiretroviral drug agent), U

$$\dot{z} = z(ex - fy) - U \quad (4)$$

to reduce the viral load. A logical first choice for U would be a positive constant. This would correspond to giving the patient a constant drug dosage. We experimented with this idea by using numerous constants in the range $[0.00001, 10.0]$. None of the constants tried in simulations were successful in reducing the viral load significantly. We then experimented with state feedback control. A simple choice for such a control is a feedback term of the form

$$U = gz \quad (5)$$

with g a constant. With this choice the system becomes simple autonomous. Therefore, the Lyapunov first method applies [17], giving the system Jacobian at the fixed point $(x_0, y_0, 0)$

$$J = \begin{bmatrix} -a & 0 & -bx_0 \\ 0 & -c & dy_0 \\ 0 & 0 & ex_0 - fy_0 - g \end{bmatrix}$$

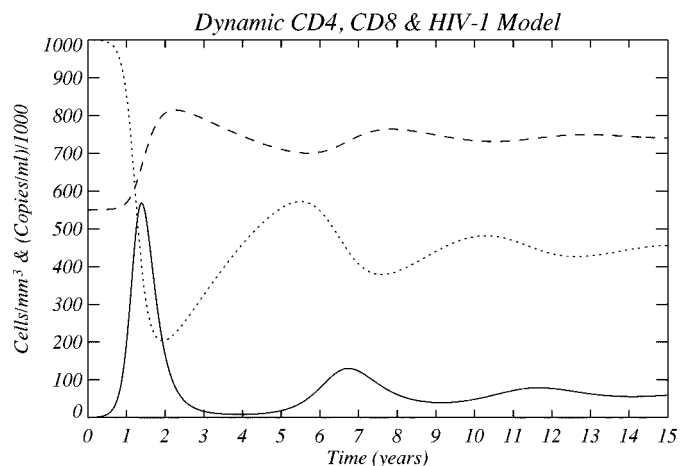


Fig. 1. Simulation of the model (1) without control. Solid line: HIV-1. Dashed line: CD8. Dotted line: CD4.

whose eigenvalues are

$$\lambda_{1,2} = -\frac{a+c}{2} \pm \frac{1}{2} \sqrt{(a+c)^2 - 4ac}, \quad \lambda_3 = ex_0 - fy_0 - g.$$

If we choose the control gain $g > (ex_0 - fy_0)$ then local stability of the controlled system about the equilibrium point $(x_0, y_0, 0)$ is guaranteed.

In order to apply feedback control of the state variables (x , y , and/or z) in a real patient they must be sampled from the blood in a periodic fashion. Realistically, such sampling can only take place at a minimum rate of about once per month (usually more like once every three months) due to the costs involved, inconvenience of the patient, etc. Based on this, a feedback controller should be implemented using a digital sampler and zero-order hold [17]. For the continuous controller $U = gz$ this becomes

$$U_d(t) = U(kt_s) = gz(kt_s) \text{ for } kt_s \leq t < (k+1)t_s, \quad (6)$$

with $t_s > 0$ the sampling period, and $k = 1, 2, 3, \dots$. The stability of this controller is dependent on the sampling period employed. A sensible approach to the design would be to minimize the mean square difference between the system under continuous control $z(t)$, and the system under discrete control $z(kt_s)$ at the sampling instants $t = kt_s$. This can be done by first designing the continuous controller U , then using a $U_d(t)$ with similar gain g for various settings of t_s to achieve stable control ($z \rightarrow 0$ as $t \rightarrow \infty$). We present simulated examples of this in what follows.

The model was simulated in the IDL language using a fifth-order Runge-Kutta approach [18] with adaptive stepsize equal to 1 week. Fig. 1 shows a simulation of a realistic case using the following values: $x_0 = 1000$ cells/mm³, $y_0 = 550$ cells/mm³, $a = 0.25$, $b = 50.0$, $c = 0.25$, $d = 10.0$, $e = 0.01$, $f = 0.006$, and the initial conditions $x = x_0$, $y = y_0$, and $z_0 = 300$ virus copies/ml at $t = 0$ (time of initial infection). Some important features of this time history are the damped oscillatory nature of the two lymphocyte populations with approximately opposite phases, and the behavior of the viral load which consists of an initial rapid rise and fall followed by a (different) oscillatory behavior.

Fig. 2(a) shows the simulation using (4) and the continuous controller

$$U = \begin{cases} 0, & \text{for } 1 > t > 9 \text{ year} \\ (ex_0 - fy_0)z, & \text{for } 1 \leq t \leq 9 \text{ year.} \end{cases} \quad (7)$$

For the initial conditions used in Fig. 1, $U(t) = 6.7z(t)$ for $1 \leq t \leq 9$ years. It can be seen that the viral load is reduced *almost* to zero during the period that $U \neq 0$. Note that the viral load spikes up again after the control is turned off with the peak occurring in year 12. Even though stability of control is guaranteed for $g > 6.7$, values of g down to about 6.0 are capable of effecting the same functional control of z to very low levels. This is because the critical value 6.7 is only sufficient but may not be necessary, as is well known from the Lyapunov first method. Fig. 2(b) shows results of the simulation using the digitally redesigned controller

$$U_d(t) = \begin{cases} 0, & \text{for } 1 > t > 9 \text{ year} \\ 6z(kt_s), & \text{for } 1 \leq t \leq 9 \text{ year} \end{cases} \quad (8)$$

with $t_s =$ eight weeks and $k = 1, 2, 3, \dots$. Note that this controller, even with a lower gain, performs as well as the continuous controller in Fig. 2(a). Fig. 2(c) shows the simulation results using $U_d(t) = 5z(kt_s)$ for $1 \leq t \leq 9$ year, $k = 1, 2, 3, \dots$, and $t_s = 12$ weeks. This example demonstrates that even a lower gain and a longer sampling period can achieve the goal of viral control.

In actual practice it may not be possible to accurately measure the parameters e , f , x_0 , and/or y_0 . This begs the question of whether there are other possibilities for U which might yield more efficient or easily implementable controls. We considered for example the following continuous time-delay feedback controller, which is a generalization of (5):

$$U(t) = g \sum_{n=0}^{N-1} z(t - n\tau) \quad (9)$$

with g constant, N is an integer number of terms in the summation, and τ is a small time delay (e.g., a day or a week). Since use of this controller leads to a nonautonomous system (it is infinite-dimensional in nature), a rigorous stability analysis should be carried out using the second Lyapunov method. For this purpose, using a simple nonsingular linear transformation,

$$\mathbf{w}(t) = [w_1(t) \ w_2(t) \ w_3(t)]^T$$

where

$$w_1(t) = x_0 - x(t), \quad w_2(t) = y_0 - y(t), \quad w_3(t) = z(t)$$

the uncontrolled system (1) is

$$\dot{\mathbf{w}} = \mathbf{f}(\mathbf{w}(t))$$

and the controlled system (1), (4), (9) can be rewritten as

$$\dot{\mathbf{w}} = \mathbf{F}(\mathbf{w}(t)) \quad (10)$$

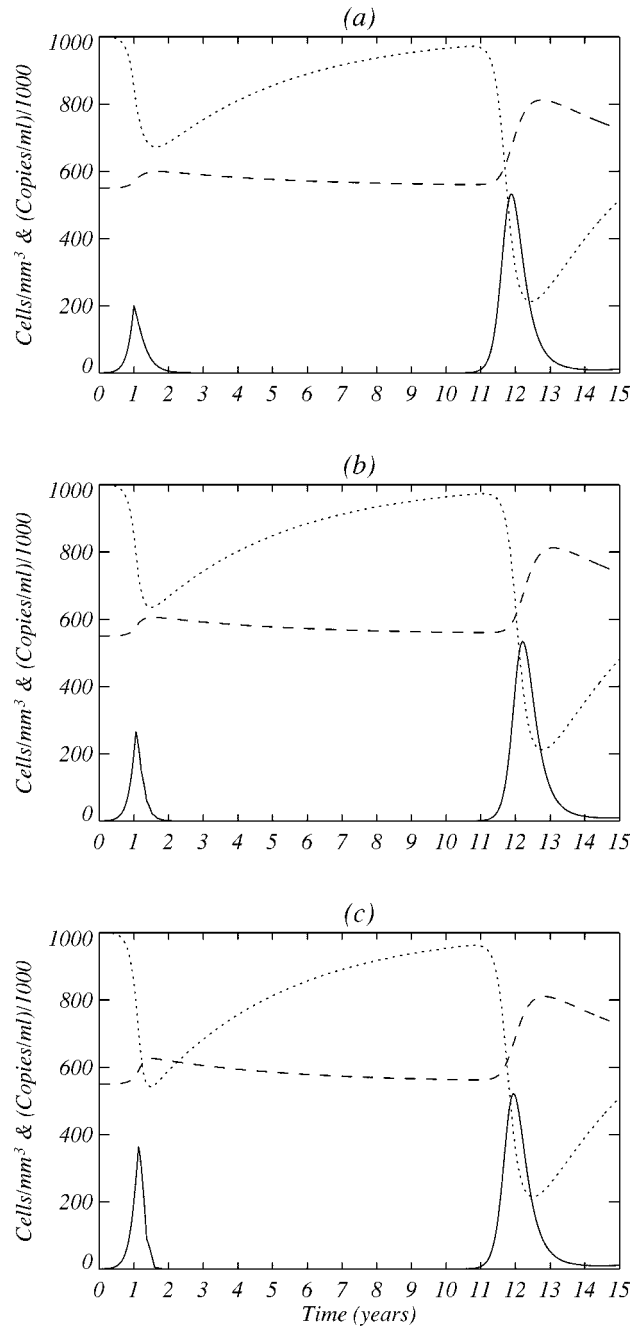


Fig. 2. Simulation of the model equations (1) and (4) with (a) continuous controller $U = 6.7z$, (b) digitally redesigned controller $U(kt_s) = 6.0z(kt_s)$ with $t_s = 8$ weeks, and (c) digitally redesigned controller $U(kt_s) = 5.0z(kt_s)$ with $t_s = 12$ weeks. Control turned on at $t = 1$ year, turned off at $t = 9$ year. All other parameters as in Fig. 1. Solid line: HIV-1. Dashed line: CD8. Dotted line: CD4.

which has a zero equilibrium point, corresponding to the original equilibrium point $(x_0, y_0, 0)$ of interest, with the notation

$$\mathbf{F}(\mathbf{w}(t)) = \mathbf{f}(\mathbf{w}(t)) + gQ(\mathbf{w}(t) - \mathbf{w}(t - \tau)) \quad (11)$$

where $Q = \text{diag}\{0, 0, 1\}$, so that here $Q\mathbf{w}(t) = [0 \ 0 \ z(t)]^T$ and $\mathbf{w}^T(t)Q\mathbf{w}(t) = z^2(t)$ in what follows below.

We now prove a local stability result. In order to simplify the notation in the following discussion and derivation, we state and prove the result for the case of a single delay only [$N = 1$ in

(9)]. On the one hand, this type of stability analysis is standard (thus, is not a focus of this paper). On the other hand, while the multiple delay case is indeed notationally more complicated than that of the single delay case, there is no qualitative difference between the two.

Theorem 1: Let J represent the constant Jacobian matrix of the controlled system (1), (4), (9), evaluated at the equilibrium point of interest. If there is a positive definite and symmetric constant matrix P and a positive constant control gain g such that the following Riccati polynomial matrix:

$$\begin{aligned} J^\top P + PJ + g^2 P Q P + g P Q + g Q P + Q, \\ Q = \text{diag}\{0, 0, 1\} \end{aligned} \quad (12)$$

is either zero or (semi)-negative definite (i.e., ≤ 0), then when $\|\mathbf{w}(t)\|$ is small enough, it will always approach zero: $\|\mathbf{w}(t)\| \rightarrow 0$ as $t \rightarrow \infty$.

Proof: We use the Lyapunov function

$$V(\mathbf{w}, t) = \mathbf{w}^\top(t) P \mathbf{w}(t) + g \int_{t-\tau}^t \mathbf{w}^\top(s) Q \mathbf{w}(s) ds. \quad (13)$$

Since zero is an equilibrium point of $\mathbf{f}(\mathbf{w}(t))$, we have a Taylor expansion $\mathbf{f}(\mathbf{w}(t)) = J\mathbf{w}(t) + [H.O.T.]$, where $[H.O.T.]$ are higher-order terms in $\mathbf{w}(t)$. Thus, we have

$$\begin{aligned} \dot{V}(\mathbf{w}, t) &= \dot{\mathbf{w}}^\top(t) P \mathbf{w}(t) + \mathbf{w}^\top(t) P \dot{\mathbf{w}}(t) + \mathbf{w}^\top(t) Q \mathbf{w}(t) \\ &\quad - \mathbf{w}^\top(t-\tau) Q \mathbf{w}(t-\tau) \\ &= [\mathbf{f}(\mathbf{w}(t)) + gQ(\mathbf{w}(t) - \mathbf{w}(t-\tau))]^\top P \mathbf{w}(t) \\ &\quad + \mathbf{w}^\top(t) P [\mathbf{f}(\mathbf{w}(t)) + gQ(\mathbf{w}(t) - \mathbf{w}(t-\tau))] \\ &\quad + \mathbf{w}^\top(t) Q \mathbf{w}(t) - \mathbf{w}^\top(t-\tau) Q \mathbf{w}(t-\tau) \\ &= [J\mathbf{w}(t) + [H.O.T.] + gQ(\mathbf{w}(t) - \mathbf{w}(t-\tau))]^\top \\ &\quad \cdot P \mathbf{w}(t) + \mathbf{w}^\top(t) P \\ &\quad \cdot [J\mathbf{w}(t) + [H.O.T.] + gQ(\mathbf{w}(t) - \mathbf{w}(t-\tau))] \\ &\quad + \mathbf{w}^\top(t) Q \mathbf{w}(t) - \mathbf{w}^\top(t-\tau) Q \mathbf{w}(t-\tau) \\ &= -[\mathbf{w}(t-\tau) + gP\mathbf{w}(t)]^\top Q [\mathbf{w}(t-\tau) + gP\mathbf{w}(t)] + \mathbf{w}^\top(t) \\ &\quad \cdot [J^\top P + PJ + g^2 P Q P + g P Q + g Q P + Q] \mathbf{w}(t) \\ &\quad + [H.O.T.]^\top P \mathbf{w}(t) + \mathbf{w}^\top(t) P [H.O.T.] < 0, \\ &\quad \forall \text{ small } \|\mathbf{w}(t)\|. \end{aligned}$$

To this end, verification using the standard class- \mathcal{K} function argument [19] of this quadratic form of the Lyapunov function for the time-delay controlled system completes the proof of the theorem.

The corresponding digitally redesigned controller is

$$U_d(t) = g \sum_{n=0}^{N-1} z(t_s[k-n]) \quad (14)$$

with $t_s > 0$ and $k = 1, 2, 3, \dots$ as before. Simulations confirm the stability of this delayed feedback digital-type controller.

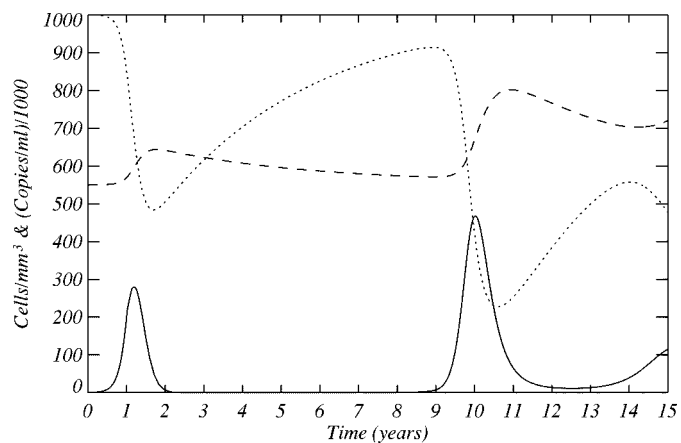


Fig. 3. Simulation of the model equations (1) and (4) with control $U(kt_s) = 1.8[z(kt_s) + z(t_s[k-1])]$, $t_s = 6$ weeks. Control turned on at $t = 1$ year, off at $t = 9$ year. All other parameters as in Fig. 1. Solid line: HIV-1. Dashed line: CD8. Dotted line: CD4.

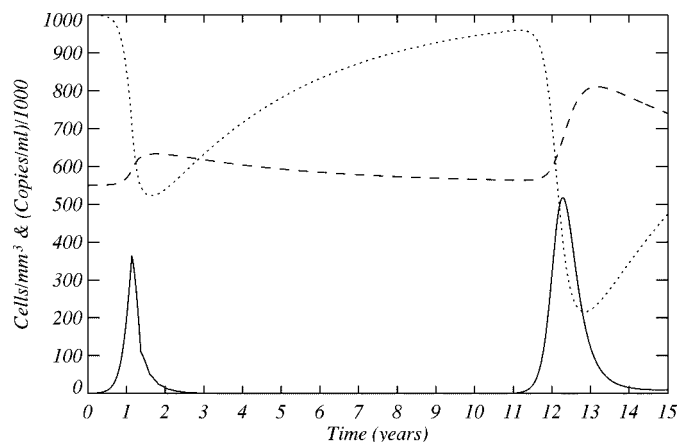


Fig. 4. Simulation of the model equations (1) and (4) with control $U(kt_s) = 4[(x(kt_s)z(kt_s))/y(kt_s)]$, $t_s = 12$ weeks. Control turned on at $t = 1$ year, off at $t = 9$ years. All other parameters as in Fig. 1. Solid line: HIV-1. Dashed line: CD8. Dotted line: CD4.

Fig. 3 is an example of use of controller (14) with $g = 1.8$, $N = 2$, and $t_s = 6$ weeks. The control is turned on at the end of year 1 and off at the beginning of year 9. The results show that the virus is reduced to almost zero as in the previous simulations. This controller would be analogous to a therapeutic regimen consisting of giving the patient a drug that is proportional to the viral load measured recently (within the last few days) and 6 weeks prior to that.

Another effective controller utilizes all three state variables (\mathbf{w}) at once and entails the following relation:

$$U_d(t) = g \sum_{n=0}^{N-1} \left[\frac{x(t_s[k-n])}{y(t_s[k-n])} \right] z(t_s[k-n]). \quad (15)$$

This design is less practical than that of (14) since all three state variables must be measured (patient CD8 cell counts are not currently routinely acquired). We present it as a fallback design if the previous designs prove ineffective. Fig. 4 shows an example of the use of this controller with $N = 1$, $g = 4$ and $t_s = 12$ weeks which achieves the control goal almost identically to the

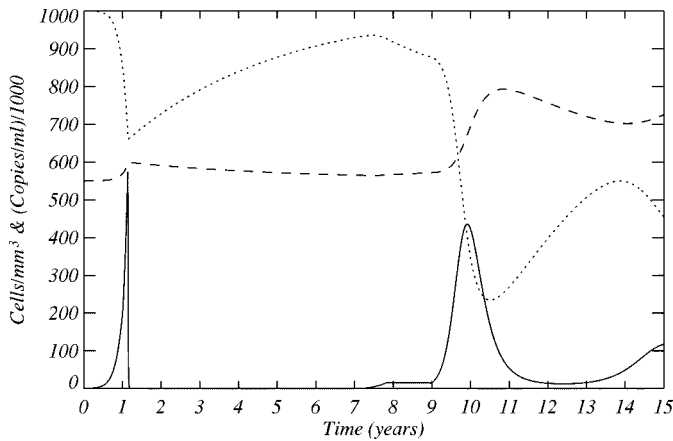


Fig. 5. Simulation of the model equations (1) and (4) with parameter feedback control $f(t_s[k+1]) = f(kt_s) + 4[(x(kt_s)z(kt_s))/y(kt_s)]$, $t_s = 12$ weeks. Control turned on at $t = 1$ year, off at $t = 9$ year. All other parameters as in Fig. 1. Solid line: HIV-1. Dashed line: CD8. Dotted line: CD4.

use of controller (14). Along similar lines, we explored the use of the following parameter feedback controller:

$$f(t_s[k+1]) = f(kt_s) + g \sum_{n=0}^{N-1} \left[\frac{x(t_s[k-n])}{y(t_s[k-n])} \right] z(t_s[k-n]) \quad (16)$$

in an effort to boost f which represents an alternative drug regimen strategy. Fig. 5 is a simple example of the use of this controller with $N = 1$, $g = 4$, and $t_s = 12$ weeks. In this case the control strategy is not as effective as the previous feedback controllers (z increases and plateaus at about 16 000 copies/ml during year seven before the control is turned off in year nine) but can still be observed to hold promise as a therapeutic drug regimen. We furthermore tested a number of feedback controllers using x alone or x and z in combination. All were either ineffective at achieving viral suppression or were unstable.

IV. CONCLUSION

We described several methods based on time-delay feedback control for stabilizing a model of HIV-1 infection. We found three highly effective controllers based on linear time delay feedback and one somewhat less effective one based on parameter time-delay feedback control. The control examples presented here were intended to provide some general guidelines that may prove helpful to clinicians and the pharmaceutical industry. The digital redesign of the continuous feedback controllers proposed here and embodied in equations (14)–(16) was based largely on empirical testing to determine how closely the performance of the redesigned controllers matched that of the continuous controllers. It should be pointed out that the stability of the redesigned controllers is dependent on the value of t_s with longer values generally associated with less stable control.

The key notion behind these simulations is that feedback control based on periodic sampling of viral load and lymphocyte counts uses a “target tracking” approach (the control U is proportional to the viral load z). Thus, the model demonstrates an

important advantage of this regimen design: once the virus is controlled to very low levels the drug dosage can be reduced proportionately. Under such circumstances side effects of the therapy will also be reduced. The potential success of this approach is the periodic modification of the antiretroviral treatment regimen similar in some ways to the infusion pump control of insulin levels in the juvenile diabetic. Perhaps in time this will lead to the development of a similar automated device for this purpose.

ACKNOWLEDGMENT

The authors would like to thank Dr. G. Wang for his invaluable technical advice and editorial suggestions.

REFERENCES

- [1] D. R. Kuritzkes. (1999) HIV pathogenesis and viral markers. *Medscape HIV Clin. Management Ser.* [Online]. Available: <http://www.medscape.com/medscape/HIV/ClinicalMgmt/CM.v02/public/index-CM.v02.html>
- [2] W. A. O'Brien, P. M. Hartigan, E. S. Daar, M. S. Simberkoff, and J. D. Hamilton, “Changes in plasma HIV RNA levels and CD4⁺ lymphocyte counts predict both response to antiretroviral therapy and therapeutic failure,” *Ann. Intern. Med.*, vol. 126, no. 12, pp. 939–945, 1997.
- [3] E. S. Rosenberg, J. M. Billingsley, A. M. Caliendo, S. L. Boswell, P. E. Sax, S. A. Kalams, and B. D. Walker, “Vigorous HIV-1—Specific CD4⁺ T cell responses associated with control of viremia,” *Science*, vol. 278, pp. 1447–1450, 1997.
- [4] A. S. Perelson, P. Essunger, Y. Cao, M. Vesanen, A. Hurley, K. Saksela, M. Markowitz, and D. D. Ho, “Decay characteristics of HIV-1-infected compartments during combination therapy,” *Nature*, vol. 387, pp. 188–191, 1997.
- [5] T. W. Schacker, J. P. Hughes, T. Shea, R. W. Coombs, and L. Corey, “Biologic and virologic characteristics of primary HIV infection,” *Ann. Intern. Med.*, vol. 128, no. 8, pp. 613–620, 1998.
- [6] M. Piatak, M. S. Saag, and L. C. Yang *et al.*, “High levels of HIV-1 in plasma during all stages of infection determined by competitive PCR,” *Science*, vol. 259, pp. 1749–1754, 1993.
- [7] D. V. Havlir and D. D. Richman, “Viral dynamics of HIV: Implications for drug development and therapeutic strategies,” *Ann. Intern. Med.*, vol. 124, pp. 984–994, 1996.
- [8] G. Pantaleo, C. Graziosi, and J. F. Demarest *et al.*, “HIV infection is active and progressive in lymphoid tissue during the clinically latent stage of disease,” *Nature*, vol. 362, pp. 355–358, 1993.
- [9] J. Embretson, M. Zupancic, and J. L. Ribas *et al.*, “Massive covert infection of helper T lymphocytes and macrophages by HIV during the incubation period of AIDS,” *Nature*, vol. 362, pp. 359–362, 1993.
- [10] J. M. Coffin, “HIV population dynamics in vivo: Implications for genetic variation, pathogenesis and therapy,” *Science*, vol. 267, pp. 483–489, 1995.
- [11] D. D. Ho, A. U. Neumann, A. S. Perelson, W. Chen, J. M. Leonard, and M. Markowitz, “Rapid turnover of plasma virions and CD4 lymphocytes in HIV-1 infection,” *Nature*, vol. 373, pp. 123–126, 1995.
- [12] A. S. Perelson, A. U. Neumann, M. Markowitz, J. M. Leonard, and D. D. Ho, “HIV-1 dynamics in vivo: Virion clearance rate, infected cell lifespan and viral generation time,” *Science*, vol. 271, pp. 1582–1586, 1996.
- [13] J. W. Mellors, A. Munoz, J. V. Giorgi, J. B. Margolick, C. J. Tassoni, P. Gupta, L. A. Kingsley, J. A. Todd, A. J. Saah, R. Detels, J. P. Phair, and C. R. Rinaldo Jr., “Plasma viral load and CD4⁺ lymphocytes as prognostic markers of HIV-1 infection,” *Ann. Intern. Med.*, vol. 126, pp. 946–954, 1997.
- [14] D. Finzi, M. Hermankova, T. Pierson, L. M. Carruth, C. Buck, R. E. Chaisson, T. C. Quinn, K. Chadwick, J. Margolick, R. Brookmeyer, J. Gallant, M. Markowitz, D. D. Ho, D. D. Richman, and R. F. Siciliano, “Identification of a reservoir for HIV-1 in patients on HAART,” *Science*, vol. 278, pp. 1295–1300, 1997.
- [15] R. Schuurman, M. Nijhuis, and R. van Leeuwen *et al.*, “Rapid changes in HIV-1 RNA load and appearance of drug-resistant virus populations in persons treated with 3TC,” *J. Infect. Dis.*, vol. 171, pp. 1411–1419, 1995.

- [16] F. M. C. de Souza, "Modeling the dynamics of HIV-1 and CD4 and CD8 lymphocytes," *IEEE Eng. Med. Biol. Mag.*, vol. 18, pp. 21–24, 1999.
- [17] G. Chen and X. Dong, *From Chaos to Order: Methodologies, Perspectives and Applications*. Singapore: World Scientific, 1998.
- [18] W. H. Press, B. P. Flannery, S. A. Teukolsky, and W. T. Vetterling, *Numerical Recipes in C*, Second ed. Cambridge, U.K.: Cambridge Univ. Press, 1992.
- [19] H. K. Khalil, *Nonlinear Systems*. New York: Macmillan, 1992.



Michael E. Brandt (S'84–M'90) received the B.S. in physics from the Polytechnic Institute of New York, Brooklyn, in 1977. He received the M.S. and Ph.D. degrees in biomedical engineering from the University of Houston, Houston, TX, in 1983 and 1989, respectively.

He was employed by Bell Laboratories, NJ from 1978–1979. From 1983 to 1989, he was a Predoctoral Research Associate in the Psychophysiology Laboratory of the University of Texas Medical Branch, Galveston, performing research in EEG and evoked potential signal analysis. In 1990, he was appointed Assistant Professor in the Department of Psychiatry, University of Texas-Houston Medical School. He was promoted to Associate Professor in 1998 and awarded tenure in 1999. In August 2000, became Associate Professor and Director of the Computational Biomedicine program in the new School of Health Information Sciences at the University of Texas Health Science Center (UTHSC). He has directed the Neurosignal Analysis Laboratory since 1990 and was recently named Director of the newly created UTHSC Center for Computational Biomedicine. He has made fundamental contributions to research in understanding the nonlinear relationship between the ongoing EEG and event-related brain potentials. Since 1990, he has worked in the area of segmentation of the brain from magnetic resonance scans in pediatric populations. His lab is currently supported by four National Institutes of Health grants studying normal and pathological brain development. He also has a great research interest in feedback control of diverse nonlinear biodynamical systems and has published extensively in this area, particularly in control of heartbeat patterns. He has written more than 50 papers, conference proceedings and book chapters and has a patent in fuzzy clustering segmentation of MR images.



Guanrong Chen (M'87–SM'92–F'96) received the M.Sc. degree in computer science from Sun Yatsen University, China, and the Ph.D. degree in applied mathematics from Texas A&M University, College Station.

Currently he is a Chair Professor in the City University of Hong Kong, Hong Kong, on leave from the position of tenured Full Professor in the Department of Electrical and Computer Engineering, University of Houston, TX. He is the (co)author of 12 research monographs and advanced textbooks, about 180 research journal papers, and 150 refereed conference papers, published since 1981 in the fields of nonlinear systems, in both dynamics and controls. Among his publications are the research monographs and edited books entitled *Hopf Bifurcation Analysis: A Frequency Domain Approach* (Singapore: World Scientific, 1996), *From Chaos to Order: Methodologies, Perspectives and Applications* (Singapore: World Scientific, 1998), and *Controlling Chaos and Bifurcations in Engineering Systems* (Boca Raton, FL: CRC, 1999). He is the Director of the Centre for Chaos Control and Synchronization at the Hong Kong City University, and is conferred the Honorary Professorship from the Central Queensland University, Australia in 2001.

Prof. Chen served and is serving as the Advisory Editor, Features Editor, and Associate Editor for six international journals including the Magazine and IEEE TRANSACTIONS ON CIRCUITS AND SYSTEMS and the *International Journal of Bifurcation and Chaos*. He received the Outstanding Prize for the Best Journal Paper Award from the American Society of Engineering Education in 1998.